European Journal of Pharmaceutics and Biopharmaceutics 135 (2019) 61–71

Contents lists available at ScienceDirect

European Journal of Pharmaceutics and Biopharmaceutics

journal homepage: www.elsevier.com/locate/ejpb

Research paper

Sustained release of recombinant thrombomodulin from cross-linked gelatin/hyaluronic acid hydrogels potentiate wound healing in diabetic mice

Yun-Yan Hsu[a,b], Kuan-Lin Liu[a], Hsun-Hua Yeh[a], Hong-Ru Lin[c], Hua-Lin Wu[b], Jui-Chen Tsai[a,*]

[a] Institute of Clinical Pharmacy and Pharmaceutical Sciences, National Cheng Kung University, Tainan, Taiwan
[b] Department of Biochemistry and Molecular Biology, National Cheng Kung University, Tainan, Taiwan
[c] Department of Chemical and Materials Engineering, Southern Taiwan University of Science and Technology, Tainan, Taiwan

ARTICLE INFO

Keywords:
Thrombomodulin
Biodegradable hydrogel
Wound healing
Diabetic mice
Stability

ABSTRACT

Thrombomodulin (TM) is a type-I transmembrane glycoprotein expressed on the surfaces of endothelial cells and epidermal keratinocytes. It is known to regulate blood coagulation, inflammation, and cell-cell adhesion. A recombinant TM, which contains an epidermal growth factor-like domain and serine/threonine-riches domain, has been demonstrated to stimulate cell proliferation and migration of keratinocytes and wound healing. In this study, we developed the biodegradable hydrogels and evaluated the efficacy of sustained release of rhTM from the hydrogel for the treatment of diabetic wounds. The hydrogels were composed of gelatin with or without hyaluronic acid, and fabricated by chemical cross-linking followed by lyophilization. Gelatin-based hydrogels had porous structure, good swelling property, and were biodegradable with characteristics of slow rhTM release in a short term. The once every-3-day rhTM-loaded hydrogel (with hyaluronic acid) markedly promoted wound healing and were superior to rhTM solution, once daily rhTM hydrogel (without hyaluronic acid), hydrogel controls, and once every-3-day rhEGF hydrogel treatment groups. The rhTM hydrogels enhanced granulation tissue formation, re-epithelialization, collagen deposition, and angiogenesis in wound repair. The once every-3-day rhTM hydrogel was stable and drug release was maintained up to 11-month of storage at 4 °C. The developed rhTM hydrogels could meet the needs for clinical practice, and may have future medical applications for wound care in diabetic patients.

1. Introduction

Cutaneous wound healing is a complex and dynamic physiological process with three phases, including inflammatory, proliferative, and tissue remodeling phases [1]. The goal of wound management and care is to heal the wound in a shortest period of time with minimum pain, reduced uncomfortable feeling and scar to patients. The global advanced wound management market was forecasted to grow at an annual growth rate of 6.25% [2]. Hydrogels are hydrophilic, insoluble and cross-linked polymer networks which are mainly made from synthetic polymers or from natural origins. The hydrogels may contain about 80%–90% water molecules when swelled in aqueous environment. By providing the moist environment inside the wound, hydrogel dressings can stimulate the growth of new tissue and the migration of epithelial cells. These benefits allow hydrogels to become the most suitable and widely used dressing for the healing process [3–5]. Wound dressings containing active ingredients such as growth factors have been applied to accelerate the healing process and to ensure the quality of recovery in clinical wound healing practice. Protein drugs can be embedded or absorbed into hydrogels, in a non-covalent or covalent way with the matrix, so that drugs can be released from the matrix through diffusion, erosion, or hydrogel degradation [6]. Compared to microspheres, lipid nanoparticles and other dosage forms, mechanical properties of hydrogels are weak. However, by selection of the material and composition, chemical modification or the use of crosslinking agent, the structure strength and pore size can be adjusted to control the drug release rate, which makes the application more flexible. Generally, natural polymers have fewer hazards related to immunological or inflammatory reactions, which may occur with synthetic polymers. Gelatin, a commonly-used natural material, is a hydrolytic product of collagen, and retains important peptide that promotes signal transfer and cell adhesion. It is economical and convenient to obtain. Hyaluronic acid (HA) is a naturally occurring polysaccharide, and also an important component of the extracellular matrix (ECM). It is reported to promote natural ECM

* Corresponding author.
E-mail address: jctsai@mail.ncku.edu.tw (J.-C. Tsai).

https://doi.org/10.1016/j.ejpb.2018.12.007
Received 30 March 2018; Received in revised form 11 July 2018; Accepted 11 December 2018
Available online 12 December 2018
0939-6411/

assembly by interacting with proteins in the physiological environment. Consequently, HA and its derivatives have been extensively studied as materials for a variety of applications in tissue engineering. 1-Ethyl-3-(3-dimethylaminopropyl) carbodiimide hydrochloride (EDC) is a widely-used, water-soluble crosslinking agent. It will link the amino and carboxyl groups in gelatin and HA to form amide and ester bonds without taking part in the linkages [6,7].

Various growth factors, cytokines and cells may contribute to the tissue repair process. To improve the healing outcome and for successful functional healing, a foundation of the interaction between cell to matrix and cell to cell for therapeutic intervention must be instilled. The balanced interaction is maintained by cytokines and growth factors. Growth factors such as epidermal growth factor (EGF), platelet-derived growth factor (PDGF), and transforming growth factor (TGF) regulate cell migration, adhesion, and proliferation to a large extent. These growth factors play a crucial role within the wound healing cascade that has the capacity to organize all events. Growth factors integrated in wound dressings as delivery systems have been applied to accelerate the healing process and to ensure the quality of recovery [8–10].

Thrombomodulin (TM) is a cell surface transmembrane glycoprotein that is expressed in a variety of cell types. Structurally, TM is composed of five domains, including an N-terminal lectin-like domain, an EGF-like domain containing six EGF-like structures, a serine/threonine-rich domain, a transmembrane domain, and a cytoplasmic domain [11]. TM can exert multiple biological functions through its different domains. TM is known to regulate blood coagulation, inflammation, and cell-cell adhesion [12–14]. Previous studies demonstrated that human recombinant TM (rhTM) containing the EGF-like domain plus the serine/threonine-rich domain stimulates cell proliferation, migration, and capillary-like tube formation in human umbilical vein endothelial cells [15]. In addition, rhTM induces angiogenesis in rat corneas and in the murine Matrigel plug assay [15]. Furthermore, recent studies showed that fibroblast growth factor receptor 1 (FGFR1) is a receptor for rhTM in angiogenesis. Local administration of rhTM enhances FGFR1 activation and increases vascular density in the rat hindlimb ischemia model [16]. These findings indicate that rhTM is a potent angiogenic factor *in vivo*.

Earlier studies revealed that TM expression is up-regulated in neoepidermis after skin wounding, and that soluble TM released by rhomboid-like-2 (RHBDL2), an intramembrane serine protease, promotes cell migration and proliferation of keratinocytes and wound healing [17]. Moreover, the epidermis-specific TM knockout mice display delayed wound healing with less neovascularization and reduced epithelial proliferation when compared to control mice [18]. The administration of rhTM improves wound repair in the TM knockout skin, in high-glucose cultured HaCaT cells and diabetic mice [18,19]. Therefore, rhTM has therapeutic potential for the treatment of skin wounds. Most of the current researches related to wound healing formulation used natural and synthetic polymers as controlled drug delivery system, usually with a degradation time up to ten days. However, it's common practice in wound care to replace the dressing and clean the wound area in a few days to ensure the effectiveness of the dressing and to prevent microbial infection. The objective of this study was to design hydrogel systems based on gelatin/HA/EDC, which would be biodegradable within a few days in the wound, as a delivery system of rhTM for chronic wound healing.

2. Materials and methods

2.1. Materials

Gelatin (G, Type A, from porcine skin), N-(3-dimethylaminopropyl)-N′-ethylcarbodiimide hydrochloride (EDC), type I collagenase (activity > 125 units/mg), bovine serum albumin (BSA), phosphate buffered saline (PBS), and streptozotocin (STZ) were purchased from Sigma-Aldrich (St. Louis, MO, USA). Hyaluronic acid (HA, sodium salt, ~1500 kDa) was obtained from SciVision Biotech Inc. (Kaohsiung, Taiwan). rhTM protein and anti-rhTM antibody were provided by Blue Blood Biotech Corporation (Taipei, Taiwan). Recombinant human epidermal growth factor (rhEGF) was obtained from Gibco® Invitrogen (Executive Way Frederick, MD, USA), and human EGF ELISA kit was from Novex® Invitrogen (Camarillo, CA, USA). Nunc-Immuno plates (MaxiSorp, 96 wells) were purchased from Nunc (Roskilde, Denmark). Tetramethylbenzidine was obtained from Clinical Science Products Inc. (Mansfield, MA, USA).

2.2. Preparation and characterization of hydrogels

2.2.1. Preparation

The preparation of hydrogels was modified from procedures described previously [20]. Gelatin and HA solutions were homogenized separately in PBS (pH 7.4). Different concentration of EDC was added to the HA solution, and the solution was mixed with an equal volume of the gelatin solution and degassed. Finally, the solution was immediately injected into glass petri dishes, and allowed to gel at room temperature. After incubation for 20 h at 4 °C to complete the cross-linking reaction, the gel was cut into 2-mm thick disks with diameter of 11 mm. The hydrogels were briefly washed three times with deionized water and lyophilized for 24 h. The dry hydrogels were stored in a desiccator until further use.

2.2.2. Scanning electron microscopy

The dried hydrogels were mounted on a conductor using a double-sided adhesive tape and sputter coated with gold using an Emitech K550 (London, England) sputter coater. A JSM-6700F (JEOL, Tokyo, Japan) scanning electron microscope operated at an accelerating voltage of 10 kV and at various magnifications was used for sample morphology observation.

2.2.3. Fourier-transform infrared spectroscopy

Hydrogel samples were milled with KBr and pressed into pellets, and analyzed by Spectrum One FT-IR spectrophotometer (Perkin Elmer Inc., USA) in the range of 4000–400 cm^{-1}.

2.2.4. In vitro water absorption

The water absorption was determined gravimetrically as described previously [21]. Hydrogels were immersed in PBS (pH 7.4) at 4 °C. At selected time intervals up to 24 h, the swelled samples were removed from PBS, wiped with tissue paper, weighed and placed again into PBS. The percentage of water absorption was calculated using the following equation, where W_S and W_0 were the weights of the swollen and dry hydrogels, respectively.

$$\text{Water absorption}(\%) = \frac{(W_s - W_0)}{W_0} \times 100\%$$

2.2.5. In vitro hydrogel degradation

In vitro degradability of the hydrogels in collagenase or PBS was investigated. Only one side of the hydrogels was exposed to 2–20 μg/mL collagenase solution or PBS at 35 °C to mimic the contact of hydrogel with wound exudate. At designated time intervals, the remaining hydrogels were removed from the solution and lyophilized for 24 h to constant weight (W_t) [22]. The dried weight loss percentage was calculated using the following equation.

$$\text{Weight loss}(\%) = \frac{(W_0 - W_t)}{W_0} \times 100\%$$

2.3. rhTM quantification

2.3.1. Indirect enzyme-linked immunosorbent assay (ELISA) of rhTM

An indirect ELISA was developed to determine the concentration of rhTM protein. Briefly, wells of a Nunc-Immuno plate were coated with 100 μL of various concentrations of rhTM standards and samples diluted in PBS containing 0.005% BSA at 4 °C overnight. The wells were washed with PBS containing 0.05% Tween 20 (PBST) and then blocked with 1% BSA in PBS at 37 °C for 1.5 h. After washing with PBST, rabbit anti-rhTM antibodies diluted in 1% BSA/PBS (1:1000) were added to the wells and incubated at 37 °C for 1.5 h. After washing four times with PBST, peroxidase-conjugated goat anti-rabbit IgG antibodies diluted in 1% BSA/PBS (1:2000) were added to the wells and incubated at 37 °C for 1 h. After washing four times with PBST, the plate was developed with 100 μL of tetramethylbenzidine substrate, and the reaction was stopped with 50 μL of 1 M H_2SO_4. The absorbance was measured at 450 nm using an ELISA plate reader.

2.3.2. Effect of collagenase treatment on indirect ELISA of rhTM

To test which condition of collagenase treatment could reduce the interference of hydrogels in indirect ELISA of rhTM, we prepared different diluents with hydrogels, which had been treated with different concentrations of collagenase and incubated for diverse times, and performed rhTM indirect ELISA. Briefly, dry hydrogels (G/HA/EDC = 4/0/0.05% w/v, abbreviated as HA(-) hydrogel) were dissolved in 1 mL of 2 or 10 μg/mL collagenase in PBS containing 0.005% BSA and incubated at 35 °C for 4 or 24 h. These solutions were further diluted 100-fold with PBS containing 0.005% BSA to make working diluents (a final concentration of 67 μg/mL gelatin). Wells of a Nunc-Immuno plate were coated with 100 μL of various concentrations (0, 5, 10, 20, 40, 80, and 160 ng/mL) of rhTM protein in different diluents overnight at 4 °C, and rhTM indirect ELISA was performed as described above.

2.4. rhTM loading and release

2.4.1. rhTM loading efficiency into hydrogels

The freeze-dried, gelatin hydrogels crosslinked with 0.05% EDC (averaged 6.7 ± 0.4 mg for HA(-) hydrogels and 6.6 ± 0.2 mg for 0.1% HA hydrogels) were impregnated with 100 μL of 30 or 90 μg/mL rhTM at 4 °C for 72 h. The swelled hydrogels were washed and then incubated in 0.9 mL of 10 μg/mL collagenase solution at 35 °C for complete degradation. The amounts of rhTM were determined by indirect ELISA. Drug loading efficiency was calculated using the equation below.

$$\text{Loading efficiency}(\%) = \frac{\text{drug amount in hydrogel}}{\text{total amount of drug added}} \times 100\%$$

2.4.2. In vitro rhTM release from hydrogels

The rhTM-loaded hydrogels were incubated in 250 μL of 2 μg/mL collagenase solution in a 24-well plate at 33 °C. At different time intervals, 20 μL of the supernatant sample was collected and replaced with the same volume of collagenase solution. The amounts of rhTM in the samples were determined by indirect ELISA, and the percentages of cumulative rhTM release were calculated.

2.5. Stability study for rhTM hydrogels

The rhTM-loaded hydrogels (G/HA/EDC = 4/0.1/0.05% w/v, abbreviated as 0.1% HA hydrogel) were tightly sealed in zip-bags individually and stored at 4 °C. After 4, 8, and 11 months of storage, rhTM content in the hydrogels and *in vitro* release were determined as described above.

2.6. Preparation and characterization of rhEGF hydrogels

100 μL of 150 μg/mL rhEGF were added to the freeze-dried 0.1% HA hydrogels at 4 °C for 72 h. Loading efficiency and *in vitro* rhEGF release from hydrogels were performed following similar procedures to rhTM. Amounts of rhEGF in the samples were determined using a commercial ELISA kit following the supplier's instruction.

2.7. Wound healing study

2.7.1. Streptozotocin-induced diabetes model

Male C57BL/6JNarl mice (8–12 weeks old, National Laboratory Animal Center, Taiwan) were housed under conditions of controlled humidity (40%) and temperature (22 ± 2 °C) with 12-hour light-dark cycles. All animal experiments were conducted in accordance with accepted standards of humane animal care, under protocols approved by the Institutional Animal Care and Use Committee (IACUC) of National Cheng Kung University. Mice were allowed free access to food and water until 4–6 h prior to streptozotocin treatment. Freshly prepared 10 mg/mL of streptozotocin in normal saline was injected intraperitoneally at 50 mg/kg to the study groups for five consecutive days. Blood glucose levels were measured using a glucose meter (BIOMINE GM550). It takes approximately 10 days after the last injection of streptozotocin until the blood glucose levels are greater than 300 mg/dL [23].

2.7.2. Wound healing experiments

Mice were anesthetized and hair on the dorsal area was removed using a depilatory cream (Nair, Church & Dwight Inc., USA) a day before the study. On the study day, a rubber O-ring (inner diameter of 12.8 mm, 2.4 mm thickness) was fixed on the dorsal midline using adhesive. An 8-mm diameter round-shaped, full-thickness excisional wound was made within the O-ring. After surgery, wound beds were rinsed with saline, and applied with different treatments immediately. Animals were housed individually and were randomly divided into seven groups: (i) PBS control, (ii) rhTM solution (3 μg), (iii) HA(-) hydrogel, (iv) HA(-) hydrogel with 3 μg rhTM, (v) 0.1% HA hydrogel, (vi) 0.1% HA hydrogel with 9 μg rhTM, (vii) 0.1% HA hydrogel with 15 μg rhEGF, and treated for six days. As shown in Fig. 1, groups i–iv were treated daily, while groups v-vii were treated once every 3 days. Tegaderm film was covered over the rubber O-ring and circumferentially around the trunk of the animal. Wound areas were photographed each day and analyzed using ImageJ 1.48 software (Nation Institutes of Health, USA) by an experienced person and verified by another. Wound area was considered as the area not covered by neoepidermis. The percentage of wound closure was calculated by the following equation.

$$\text{Wound Closure}(\%) = \frac{\text{Wound Area}_{\text{Day1}} - \text{Wound Area}_{\text{Day n}}}{\text{Wound Area}_{\text{Day1}}} \times 100\%$$

Hydrogel degradation on the wounds was evaluated during the wound healing process. The scoring method is as follows: score 5, entire hydrogel with no or little degradation (< 20% degradation); score 4, entire but thinner hydrogel (20–40% degradation); score 3, about half of hydrogel existed (40–60% degradation); score 2, small piece of hydrogel remained (60–80% degradation); score 1, most hydrogel disappeared (> 80% degradation); score 0, no hydrogel existed (100% degradation).

2.7.3. Histology and Masson's trichrome staining

On day 10, the animals were sacrificed, and wounded skins were collected and fixed in 4% paraformaldehyde [24,25]. After routine processing and embedding in paraffin, 5 μm-thick sections were cut and stained with hematoxylin and eosin for general observation of skin layers. For Masson's trichrome staining to assess the extent of collagen deposition, skin wound sections were deparaffinized in xylene,

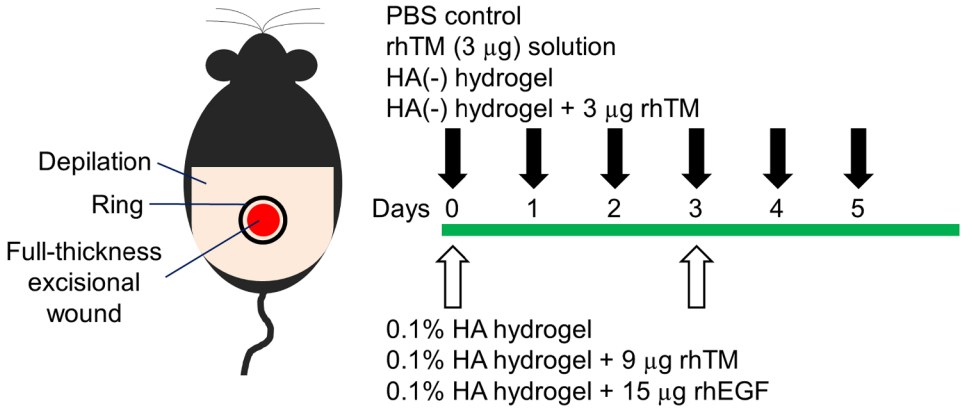

Fig. 1. Topical treatment protocol. On day 0, a full-thickness excisional wound was created within a rubber O-ring that was fixed on the back of streptozotocin-induced diabetic mice. The black arrows denote the application days for PBS control, rhTM (3 μg) solution, HA(-) hydrogel and HA(-) hydrogel + 3 μg rhTM. The white arrows represent the application days for 0.1% HA hydrogel, 0.1% HA hydrogel + 9 μg rhTM and 0.1% HA hydrogel + 15 μg rhEGF.

rehydrated in a graded series of ethanol (95, 90, 80, 70, and 60%), and washed in deionized water. Masson's trichrome staining was performed using a Masson's trichrome staining kit (HT15; Sigma-Aldrich, St. Louis, MO, USA). The sections were incubated in Bouin's solution (HT10132; Sigma-Aldrich) at 56 °C for 1 h and then washed in tap water for 5 min. They were then stained with Weigert's iron hematoxylin (HT107, HT109; Sigma-Aldrich) for 10 min, washed in running water for 5 min, and rinsed in deionized water. The sections were stained with Biebrich Scarlet-Acid Fuchsin for 5 min. After washing with deionized water, the sections were incubated with phosphotungstic/phosphomolybdic acid solution for 10 min and stained with aniline blue solution for 5 min. Followed by differentiation in 1% (v/v) acetic acid for 2 min and rinsed in deionized water, the sections were dehydrated in 95% ethanol for 1 min and in xylene for 10 min, and mounted with mounting media (Surgipath Micromount, Leica Biosystems, Richmond, IL, USA). The sections were photographed using an Olympus BX50 microscope (Olympus, Tokyo, Japan).

2.7.4. Immunofluorescence staining

Mouse skin wound tissue was excised, embedded in OCT (Sakura), frozen in liquid nitrogen, and stored at −70 °C. The skin wound specimens were cut at 4 μm thickness, and the tissue sections on slides were air dried for 30 min and fixed in ice-cold acetone for 5 min. After washing with PBS, the sections were blocked with 5% normal goat serum (blocking solution) for 2 h at room temperature, and then incubated with primary antibody rat anti-mouse CD31 (553370; BD Biosciences Pharmingen; 1 : 100 in blocking solution) for 2 h at room temperature. The sections were washed with PBST, and then incubated with secondary antibody Alexa Fluor 546-conjugated goat anti-rat IgG (Invitrogen; 1 : 200 in blocking solution) for 1.5 h at room temperature. The nuclei were counterstained with 4′,6-diamidino-2-phenylindole (DAPI, Sigma-Aldrich; 0.2 μg/mL DAPI in PBS) for 5 min at room temperature. After washing with PBST, the sections were mounted with Fluoromount-G (Southern Biotech, Birmingham, AL). Images were acquired using an Olympus BX50 microscope.

2.8. Statistical analysis

The results of *in vitro* studies were expressed as the means ± standard deviation (SD), and the *in vivo* data were presented as the means ± standard error of the mean (SEM). General linear model (GLM) was used for analysis of multiple comparisons of wound healing effect between groups. The means were compared through student's *t* test or one-way ANOVA for multiple comparisons. Differences were considered statistically significant at $p < 0.05$. All of the computations were performed using SPSS 17.0 (SPSS, Inc., Chicago, IL, USA).

3. Results and discussion

3.1. Characterization of hydrogels

3.1.1. Morphology of hydrogels

SEM revealed hydrogels prepared using 4% (w/v) type A gelatin, 0–0.15% (w/v) HA, and cross-linked with 0.025–0.1% EDC were porous (approximately 20–300 μm in diameter). Gelatin alone is able to form porous structure. With the increase of HA and EDC concentrations, the pore size of the crosslinked hydrogels of gelatin has a narrowing trend (Supplementary Fig. S1 and Fig. 2A). Hydrogel of HA/EDC = 0.15/0.1 (% w/v) composition showed smallest pore size (Supplementary Fig. S1, p).

3.1.2. FTIR analysis

The FTIR spectra of gelatin, HA and the hydrogels are presented in Fig. 2B. In the spectrum of pure HA (Fig. 2B, a), the peak at 1048 cm^{-1} referred to the C—O—C stretching. The absorption peaks at 1417 cm^{-1} and 1614 cm^{-1} corresponded to carboxyl groups for the symmetric and asymmetric stretching vibration bands. The peaks at 1650 cm^{-1} and 1545 cm^{-1} in the spectrum of pure gelatin (Fig. 2B, b) were attributed to amide I for C═O stretching vibration and amide II for N—H bending vibration, respectively. In addition, the peaks at 1455 cm^{-1} and 1081 cm^{-1} corresponded to the C—H bending and the C—O stretching, respectively. The spectra of the hydrogels were characterized by the presence of the amide bands (1650 cm^{-1} and 1545 cm^{-1}) and the peaks at 1455 cm^{-1} and 1081 cm^{-1} (Fig. 2B, c–f). Due to the low concentration of HA (0.15%), the peak at 1048 cm^{-1} (C—O—C stretching) was small in the spectra of the hydrogels (Fig. 2B, e and f). Typical FTIR absorption peaks of both gelatin and HA were observed in the spectra of the hydrogels.

EDC has been widely used to cross-link protein and polysaccharide by triggering the amide/ester bond formation between their side groups. EDC has the ability to react with carboxyl groups of gelatin or HA to yield activated intermediates. The intermediates can further react with amino groups of gelatin to form amide bonds, or with hydroxyl groups of HA to form ester bonds. Therefore, EDC can lead to gelatin–gelatin, gelatin–HA, and HA–HA cross-linking [7,20,26]. Since amide groups and C–O bonds exist in the structure of gelatin and HA, the absorption peaks of newly formed amide groups (1650 cm^{-1} and 1545 cm^{-1}) and ester bonds (1081 cm^{-1}) through EDC cross-linking overlapped with that of gelatin and HA. Thus, no new absorption peaks appeared in the spectra of cross-linked hydrogels.

3.1.3. Water absorption

The water absorption profiles of hydrogels are shown in Fig. 2C and Supplementary Fig. S2. The water absorption increased rapidly within the initial 30 min, and the hydrogels swelled more than 11-fold within 24 h. It was found that water absorption of the hydrogels decreased

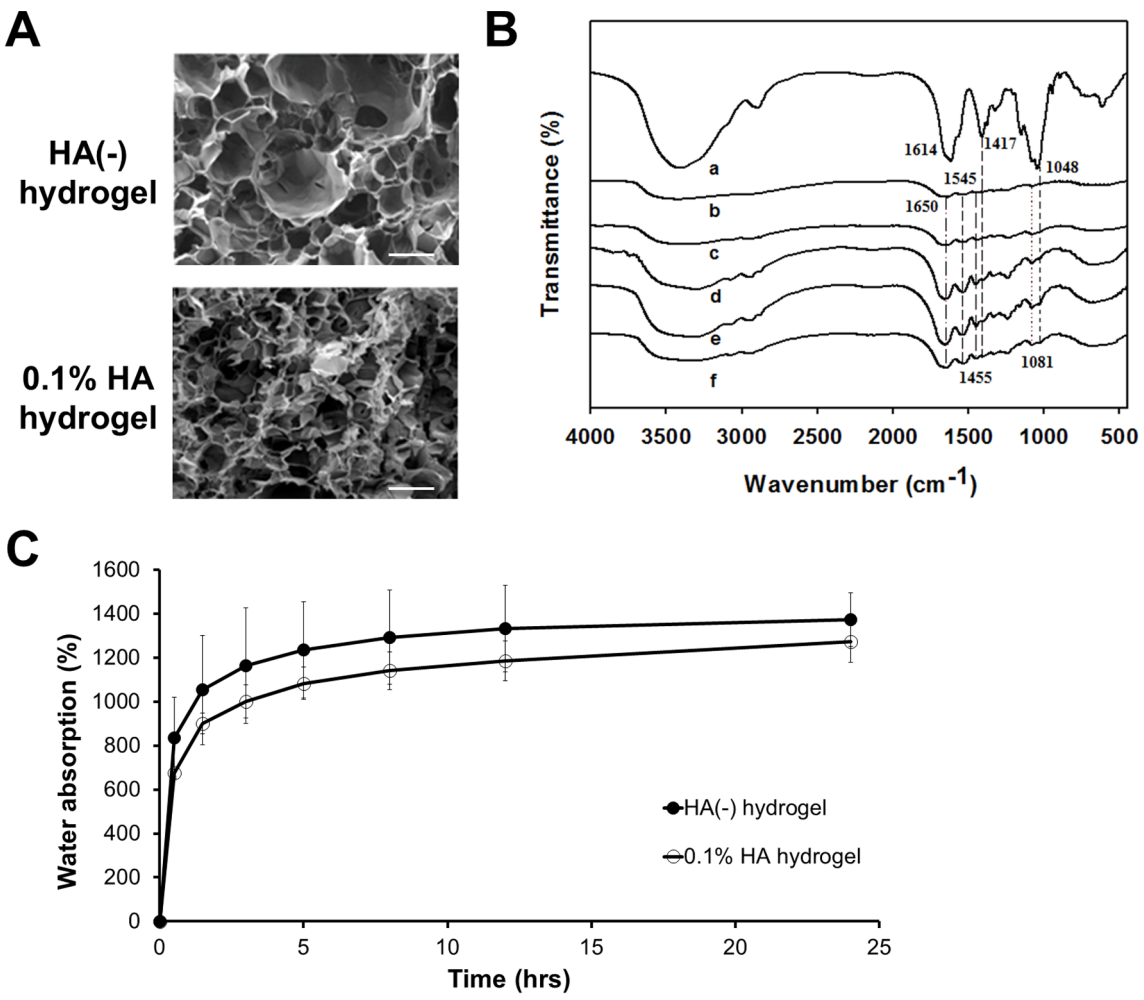

Fig. 2. Characterization of hydrogels. (A) SEM micrographs of cross-linked gelatin hydrogels (cross-section). Scale bars = 200 μm. (B) FTIR spectra of the hydrogels and raw materials. (a) Hyaluronic acid, (b) Gelatin, (c) G-HA-EDC (4-0-0.05), (d) G-HA-EDC (4-0-0.1), (e) G-HA-EDC (4/0.15/0), (f) G-HA-EDC (4/0.15/0.1). (C) In vitro water absorption profile of cross-linked gelatin hydrogels in PBS at 4 °C. Data are presented as mean ± SD (n = 3).

with increasing concentration of EDC. HA did not obviously affect the water absorption properties of hydrogels. Taken together, all the hydrogels have good water absorption behavior, which may be beneficial for drug absorption, absorbing exudates and providing moisture environment for wound bed.

3.1.4. *In vitro degradation of hydrogels*

The wound exudates and tissues have been shown to contain collagenases, which are produced by inflammatory cells and fibroblasts [27–29]. To assess the biodegradability of hydrogels under the condition that mimics the wound environment, we performed *in vitro* degradation studies of the hydrogels in collagenase solution. Different concentrations of collagenase have been reported in previous studies for hydrogels prepared with higher concentrations of cross-linking agent [22,26,30]. To determine appropriate enzyme concentration to mimic enzyme content in the wound exudates, two formulations of hydrogels (containing 0.1% HA and crosslinked with 0.05% or 0.1% EDC) were selected to examine their *in vitro* degradation in 2–20 μg/mL collagenase at 35 °C. As shown in Supplementary Fig. S3, the higher concentration of collagenase resulted in faster degradation of the hydrogels. Since the hydrogels degraded too quickly in 5–20 μg/mL collagenase solutions, further degradation studies for hydrogels with different compositions were carried out in 2 μg/mL collagenase solution and PBS.

The hydrogels with 0.025% EDC were rapidly degraded in 2 μg/mL collagenase within 3–6 h, while the hydrogels with 0.05% EDC were completely degraded after 6–12 h (Supplementary Fig. S4). In contrast, hydrogels with 0.1% EDC were gradually degraded in 2 μg/mL collagenase in a 24-hour period. Hydrogels with 0.025% EDC were rapidly degraded in PBS within 3–6 h (Supplementary Fig. S5). These findings suggest that EDC concentrations used for hydrogel preparation should be greater than 0.025% to maintain the hydrogel structures for longer periods. Particularly, the hydrogels with 0.05% EDC were degraded in a HA-dependent manner within 24–72 h. In contrast, the degradation of the hydrogels with 0.1% EDC was less than 30% after incubation in PBS for 72 h.

Fig. 3A shows the weight loss percentage of HA(-) and 0.1% HA hydrogels (both crosslinked with 0.05% EDC) in 2 μg/mL collagenase solution after 3-hour incubation was about 60% and 45%, respectively. Although the degradation of the 0.1% HA hydrogels was slower than that of the HA(-) hydrogels, both hydrogels were completely degraded in 2 μg/mL collagenase solution within 12 h. The degradation profiles of the HA(-) and 0.1% HA hydrogels in PBS were shown in Fig. 3B. The HA(-) hydrogels were degraded rapidly in PBS within 24 h, whereas the 0.1% HA hydrogels were degraded in PBS slowly and gradually within 72 h. This means that the degradation rate of the 0.05% EDC hydrogels in PBS decreased significantly with the presence of 0.1% HA. These results indicate that the hydrogels are degradable in collagenase and PBS, and the degradation rate is associated with the concentrations of HA and EDC. However, it should be noted, in the current setting to measure hydrogel degradation, weight loss may be partly attributed to the dissolution of free gelatin and HA in the hydrogel, especially in the case of PBS.

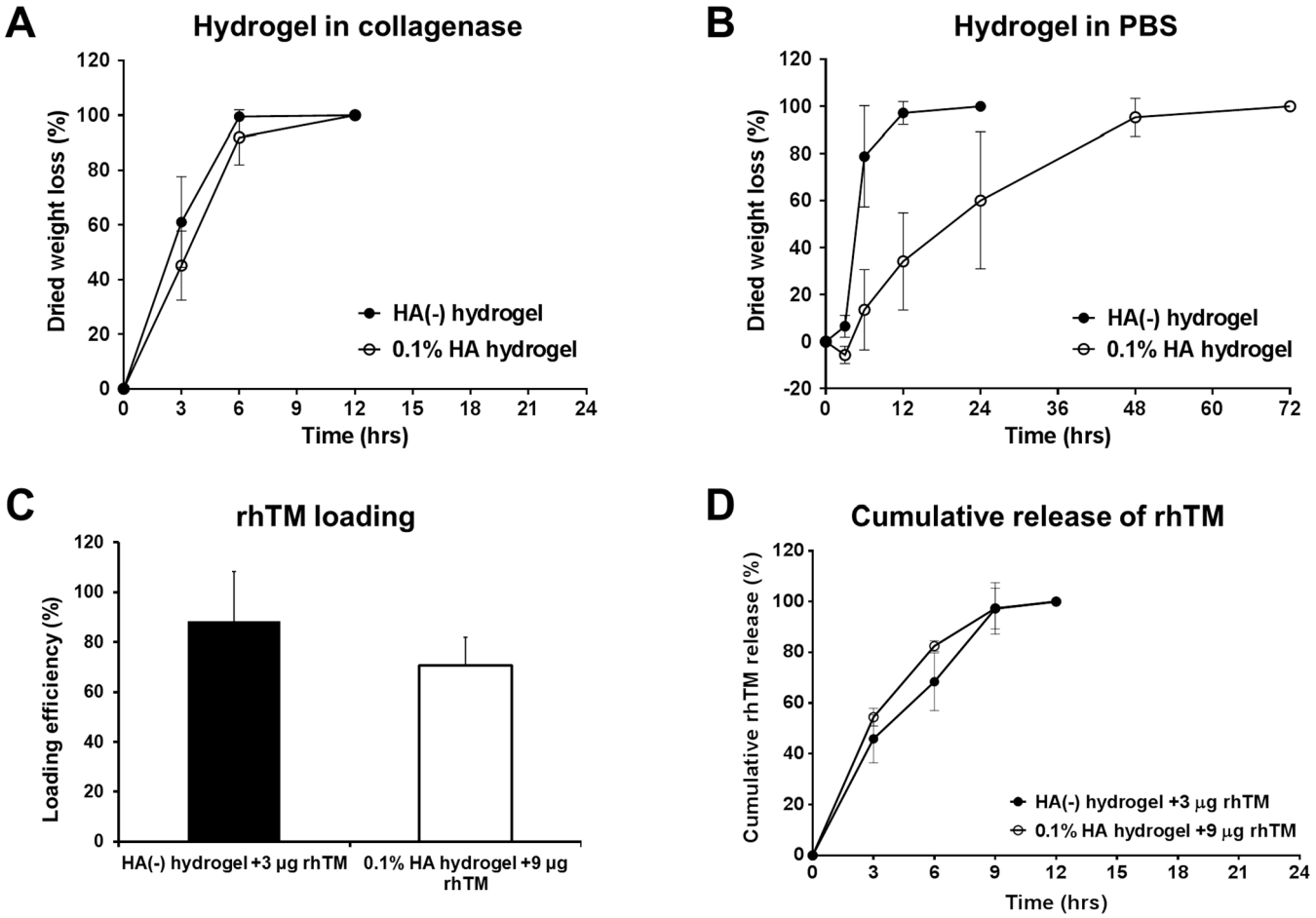

Fig. 3. In vitro degradation profiles of cross-linked gelatin hydrogels in (A) 2 μg/mL collagenase solution and (B) PBS (pH 7.4) at 35 °C. (C) Loading efficiency of rhTM in hydrogels. (D) Percentages of cumulative rhTM release from hydrogels in 2 μg/mL collagenase solution at 33 °C. Data are presented as mean ± SD (n = 3).

3.2. Effect of hydrogels on rhTM quantification

Since gelatin, the major component of hydrogels, is a protein, hydrogels dissolved in buffer may be absorbed onto ELISA plate wells. It is possible that gelatin in dissolved hydrogels may affect the coating of rhTM protein on plate wells when the rhTM indirect ELISA is performed. It appeared that hydrogel diluent decreased the response of spiked rhTM protein detected by indirect ELISA (data not shown). When the hydrogels were treated with 2 μg/mL collagenase for 4 or 24 h and further diluted 100-fold, the partially digested hydrogels decreased the indirect ELISA response in comparison with the response of rhTM in the diluent with 0.005% BSA alone (Supplementary Fig. S6). After the hydrogel was treated with 10 μg/mL collagenase for 24 h, the extensively digested hydrogel did not interfere with rhTM quantification (Supplementary Fig. S6). Therefore, collagenase treatment to completely digest hydrogels can reduce the interference of hydrogels on rhTM indirect ELISA. When the standards of rhTM were in the range of 10 to 160 ng/mL dissolved in the diluents with or without extensively degraded hydrogel, the inter-assay coefficient of variation (CV) was 8.0–24.0% and 1.3–19.1%, respectively (n = 11). Consequently, samples from rhTM loading efficiency and *in vitro* release experiments were pretreated with 10 μg/mL collagenase at 35 °C for 24 h prior to indirect ELISA analysis.

3.3. rhTM loading efficiency and in vitro release

HA(-) and 0.1% HA hydrogels were impregnated with 100 μL of 30 and 90 μg/mL rhTM solutions, respectively. The rhTM loading efficiencies of HA(-) hydrogel with 3 μg rhTM and 0.1% HA hydrogel with 9 μg rhTM were 88.3 ± 20.0% and 70.7 ± 11.3%, respectively (Fig. 3C). Loading efficiency of rhTM was higher in the HA(-) hydrogel than in the 0.1% HA hydrogel. An explanation for the difference in loading is that the HA (-) hydrogel with larger pores absorbs more rhTM solution than the 0.1% HA hydrogel with smaller pores. Loading efficiency of 0.1% HA hydrogel with 15 μg rhEGF was 73.2 ± 0.8%, similar to 0.1% HA hydrogel with 9 μg rhTM.

The release profiles of rhTM from HA(-) hydrogels and 0.1% HA hydrogels in 2 μg/mL collagenase solution at 33 °C are shown in Fig. 3D. Both hydrogels showed fast release of rhTM (> 40%) in the first 3 h and sustained release thereafter. rhTM was fully released from the hydrogels within 12 h. However, there was no significant difference between the release profiles of rhTM from both hydrogels under the *in vitro* condition. Similar release profile of rhEGF from hydrogels was also observed (data not shown).

3.4. Stability of rhTM hydrogels

The content of rhTM in 0.1% HA hydrogel after storage for 4, 8, and 11 months was 98.7 ± 22.8, 121.2 ± 11.5, and 107.6 ± 45.0% of initial content (0 month), respectively. In addition, after 4, 8, and 11 months of storage, the release profiles of rhTM from hydrogels did not show appreciable differences from that at 0 month (Supplementary Fig. S7). These data indicate that 0.1% HA hydrogel with 9 μg rhTM was stable at 4 °C for at least 11 months, and rhTM can be released from the hydrogels after long-term storage.

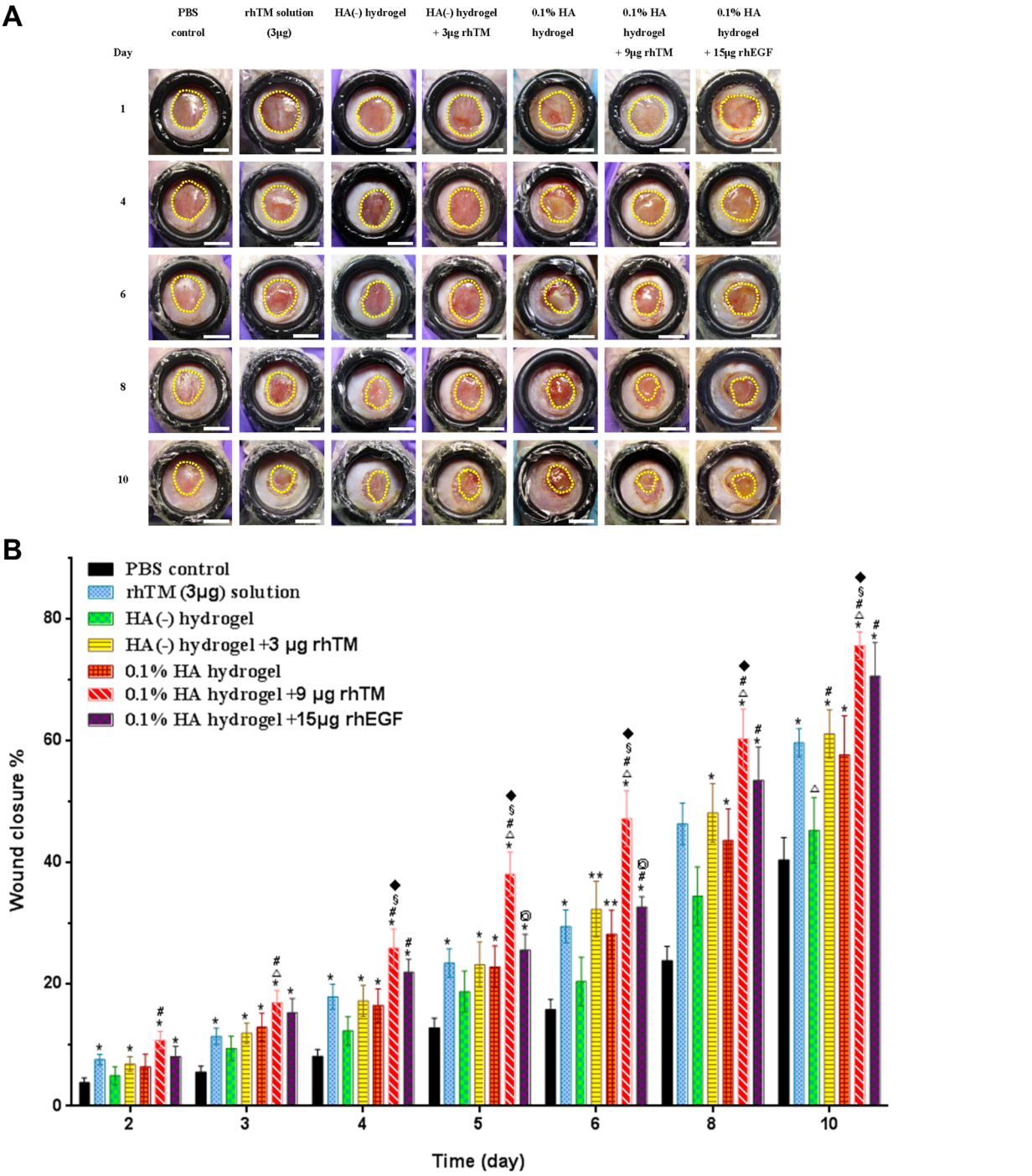

Fig. 4. Cross-linked gelatin/hyaluronic acid hydrogel enhances the therapeutic efficacy of rhTM in diabetic wounds. (A) Representative images of wound closure in diabetic mice treated with PBS, rhTM solution (3 μg), HA(-) hydrogel, HA(-) hydrogel + 3 μg rhTM, 0.1% HA hydrogel, 0.1% HA hydrogel + 9 μg rhTM, or 0.1% HA hydrogel + 15 μg rhEGF. Scale bars = 5 mm. (B) Percentages of wound closure relative to the initial wound area on day 1 in diabetic mice with different treatments. Data are presented as mean ± SEM (n = 9–13). The statistical significance was analyzed using Student's *t*-test. *Significantly different from PBS control group ($p < 0.05$). △Significantly different from rhTM solution group ($p < 0.05$). #Significantly different from HA(-) hydrogel group ($p < 0.05$). §Significantly different from HA(-) hydrogel + 3 μg rhTM group ($p < 0.05$). ◆Significantly different from 0.1% HA hydrogel group ($p < 0.05$). ©Significantly different from 0.1% HA hydrogel + 9 μg rhTM group ($p < 0.05$).

3.5. Wound healing effect in diabetic mice

3.5.1. rhTM hydrogels accelerated wound healing in diabetic mice

The wound healing experiments were conducted on streptozotocin-induced diabetic mice. The major mechanism of wound closure in mice is wound contraction, while the major mechanisms of wound closure in humans are re-epithelialization and granulation tissue formation [31,32]. To prevent wound contraction and mimic the process of human wound healing, we have developed a simplified splinted skin wound healing model by using an O-ring to fix the skin around the wound opening. Based on the results of *in vitro* studies, the two hydrogels (HA(-) hydrogel with 3 μg rhTM and 0.1% HA hydrogel with 9 μg rhTM) with good water absorption ability, more than 70% of drug loading, and sustained release pattern in a short term, were selected to evaluate their *in vivo* wound healing effect. Wound closure was monitored for 10 days after wounding shown in Fig. 4A. The percentages of

Table 1
Multiple comparison analysis of wound healing effect between groups based on general linear model. The Bonferroni post hoc test was applied. (N = 9–13 each group).

	PBS control	rhTM (3 μg) solution	HA(-) hydrogel	HA(-) hydrogel +3 μg rhTM	0.1% HA hydrogel	0.1% HA hydrogel +9 μg rhTM	0.1% HA hydrogel +15 μg rhEGF
PBS control	—						
rhTM (3 μg) solution	*	—					
HA(-) hydrogel	ns	*	—				
HA(-) hydrogel +3 μg rhTM	*	ns	*	—			
0.1% HA hydrogel	*	ns	*	ns	—		
0.1% HA hydrogel +9 μg rhTM	*	*	*	*	*	—	
0.1% HA hydrogel +15 μg rhEGF	*	ns	*	ns	*	*	—

*: $p < 0.05$.
ns: $p > 0.05$.

wound closure were calculated and plotted (Fig. 4B). The general linear model was used for multiple comparison analysis of wound healing effects between groups, and results are shown in the Table 1 Compared with PBS control, treatment with rhTM solution (3 μg) significantly accelerated wound closure in the diabetic mice from day 2 to day 10 ($p < 0.05$). The once daily (no HA) hydrogel slightly increased wound closure ($p > 0.05$), whereas the once every-3-day (0.1% HA) hydrogel obviously enhanced wound healing and was as good as rhTM solution (3 μg). The healing effect of once daily hydrogel with 3 μg rhTM was similar to that of rhTM solution (3 μg). The once every-3-day hydrogel with 9 μg rhTM markedly promoted skin wound healing in comparison with PBS control ($p < 0.05$), and was superior to all the other treatment groups including once every-3-day hydrogel with 15 μg rhEGF ($p < 0.05$). Once every-3-day hydrogel with 15 μg rhEGF demonstrated significantly more healing effect than hydrogel alone, but its effect did not differ from rhTM solution (3 μg) and once daily hydrogel with 3 μg rhTM ($p > 0.05$). These results suggest that, not only rhTM has synergistic healing effect with HA-containing hydrogels, but also its effect is more potent than rhEGF. Previous studies showed that HA and HA-based dressings have the ability to enhance wound healing in diverse animal models and diseases [33,34]. Indeed, the healing was faster in the mice treated with the once every-3-day hydrogel compared to those treated with the once daily hydrogel ($p < 0.05$). It is also likely that less frequent application of hydrogel (once every-3-day vs. daily) minimizes the destruction of neo-epidermis. These results indicate that the cross-linked gelatin/HA hydrogel is an excellent topical delivery system for rhTM to enhance wound healing.

3.5.2. *In vivo hydrogel degradation on wounds*

During the wound healing studies, degradation of hydrogels *in vivo* was also assessed. As shown in Supplementary Fig. S8, once daily hydrogels and once every-3-day hydrogels were biodegradable on the excisional wounds of diabetic mice. The remaining hydrogels of once daily hydrogels (with and without rhTM) were decreased from day 1 to day 6 (Supplementary Fig. S9, the bar graph), suggesting that the degradation rate was increased with treatment days on the wounds. On the other hand, the remaining hydrogels of once every-3-day hydrogels (with and without rhTM) were diminished after 3 days (Supplementary Fig. S9, day 3 and day 6 of the line gragh), and the degradation rate of the second application (day 4) appeared to be faster than the first application (day 1). Hydrogel degradation was not affected by rhTM loading. The results indicate that the hydrogels are slowly degraded on skin wounds and may release the drug (rhTM) in a sustained way. The *in vivo* hydrogel degradation on wounds was slower than the *in vitro* hydrogel degradation in PBS and collagenase solution. An explanation is that the amount of the wound exudates and proteases was few in the skin wound model.

3.5.3. *Histological examination*

In the new tissue formation phase of skin wound repair, immune cells are present and new blood vessels develop at the wound site [1]. Fibroblasts can migrate into the wound, proliferate, and produce the extracellular matrix, including collagen [35], forming granulation tissue [36]. In addition, keratinocytes at the wound edge migrate and highly proliferate to form a new epidermis that covers the wound, the so-called wound re-epithelialization [36]. Both granulation tissue formation and re-epithelialization contributes to wound healing [1]. The H &E and Masson's trichrome staining of both the central wound areas and wound edges collected from diabetic mice at day 10 after injury were shown in Fig. 5A and B, respectively. H&E staining revealed a thin granulation tissue in the PBS control group (Fig. 5A, a). In contrast, thick granulation tissues and increased re-epithelialization were observed in rhTM solution (3 μg), HA(-) hydrogel, HA(-) hydrogel with 3 μg rhTM, 0.1% HA hydrogel, and 0.1% HA hydrogel with 9 μg rhTM groups (Fig. 5A, b–f).

Masson's trichrome staining is a method to detect collagen expression. The originally deposited collagen in the skin was seen in deep blue (Fig. 5, asterisks), and the newly formed collagen was seen in faint blue (Fig. 5, arrows). Masson's trichrome staining displayed few collagen fibers that form in the granulation tissue of PBS-treated mice (Fig. 5A and B, g). Similarly, few collagen fibers were present in the wounds of mice treated with HA(-) hydrogel or 0.1% HA hydrogel (Fig. 5A and B, i and k). Notably, treatments with rhTM solution (3 μg), HA(-) hydrogel with 3 μg rhTM, or 0.1% HA hydrogel with 9 μg rhTM increased collagen deposition (blue staining) in the granulation tissue (Fig. 5A and B, h, j, and l, arrows).

Following skin injury, PDGF and TGF-β are released to stimulate fibroblast proliferation in granulation tissue [35]. Furthermore, fibroblasts synthesize and secrete collagen to the extracellular space [35,37]. A previous study reported that the recombinant TM protein containing the EGF-like domain induces proliferation of the Swiss 3 T3 fibroblast cell line [38]. Here, we found that rhTM and rhTM-loaded hydrogels increased granulation tissue formation and collagen expression, and 0.1% HA hydrogel with 9 μg rhTM had higher potency. These results suggest that rhTM-loaded hydrogels enhance fibroblast proliferation and collagen synthesis, thus facilitating wound healing.

3.5.4. *Evaluation of wound angiogenesis*

Angiogenesis, the growth of new vessels from pre-existing vessels, is a crucial step in the wound healing process [39–41]. CD31 (platelet endothelial cell adhesion molecule-1; PECAM-1) is an integral membrane glycoprotein highly expressed on endothelial cells [42]. The staining of CD31 can be used to evaluate the formation of new blood vessels (neovascularization) [43,44]. To examine angiogenesis in wounds after the treatment, we collected wounded skins from diabetic mice at day 10 after wounding and carried out immunostaining for CD31. As shown in the representative images, rhTM solution (3 μg),

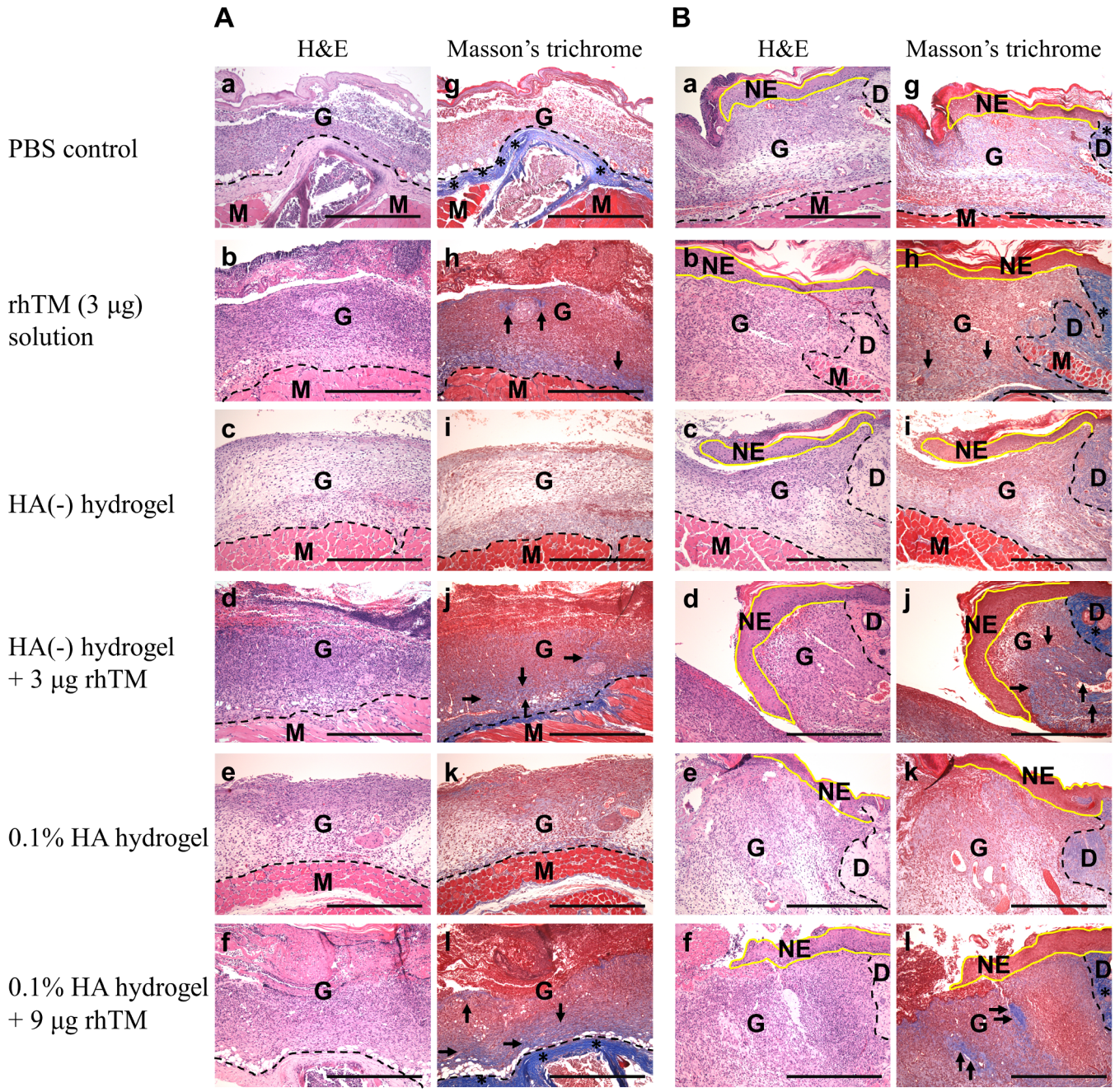

Fig. 5. Cross-linked gelatin hydrogels loaded with rhTM increase collagen deposition at the wound site. (A and B) Representative images of hematoxylin and eosin (H &E) staining (a–f) and Masson's trichrome staining (g–l) of skin wound sections at day 10 after wounding from diabetic mice with indicated treatments. (A) The central areas of the wounds are shown. (B) The wound areas adjacent to the wound edge are shown. Asterisks denote originally deposited collagen (deep blue), not newly formed collagen. Masson's trichrome staining demonstrates elevated collagen expression (arrows, blue staining) in the granulation tissue of wounds treated with rhTM solution (3 μg), HA(-) hydrogel + 3 μg rhTM, or 0.1% HA hydrogel + 9 μg rhTM. Yellow lines denote neo-epidermis. Dashed lines denote boundaries between the granulation tissue and dermis/muscle. G, granulation tissue; NE, Neo-epidermis; D, dermis; M, muscle. Scale bars = 500 μm. (For interpretation of the references to colour in this figure legend, the reader is referred to the web version of this article.)

HA(-) hydrogel with 3 μg rhTM, and 0.1% HA hydrogel with 9 μg rhTM obviously induced angiogenesis in the granulation tissue of wounded skins from diabetic mice at day 10 (Fig. 6). Previous studies showed that rhTM containing the EGF-like domain plus the serine/ threonine-rich domain (TMD23) is an angiogenic factor, which induces angiogenesis in rat corneas and in the murine Matrigel plug assay [15]. TMD23 induces cell proliferation, migration, and tube formation of human umbilical vein endothelial cells [15]. In this study, we found that more blood vessels were present in the granulation tissue of skin wounds treated with rhTM solution and rhTM-loaded hydrogels. Notably, the rhTM-loaded hydrogels induced more angiogenesis than rhTM alone. These results indicate that rhTM-loaded hydrogels enhance wound angiogenesis, thereby promoting skin wound healing.

4. Conclusion

In this study, we developed the biodegradable hydrogels and evaluated the efficacy of sustained release of rhTM from the hydrogel for the treatment of diabetic wounds. The developed gelatin-based hydrogels were biodegradable on skin wounds and could slowly release rhTM

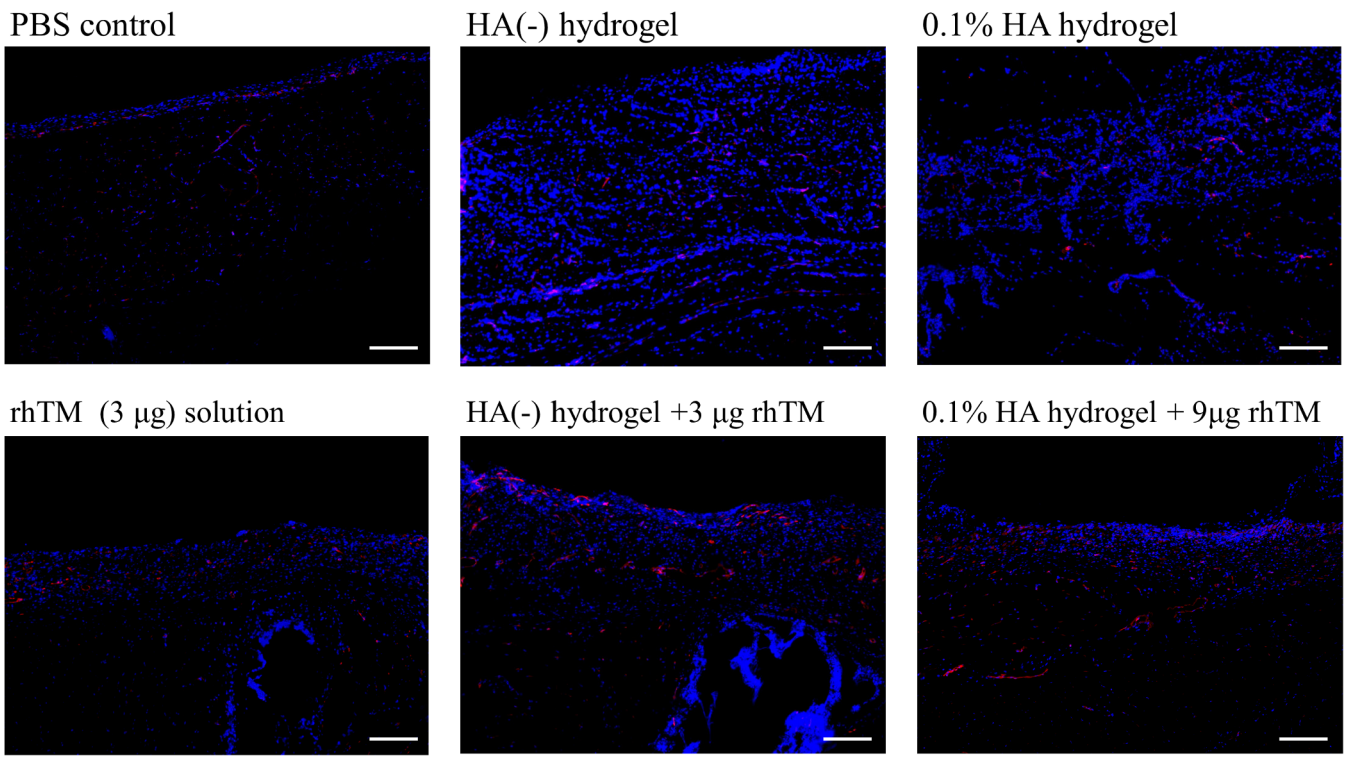

Fig. 6. Cross-linked gelatin hydrogels loaded with rhTM promote wound angiogenesis. Shown are representative immunofluorescence images of wounds at day 10 in diabetic mice with indicated treatments. Skin wound sections were immunostained for CD31 (red) to detect new blood vessels and co-stained with DAPI (blue) to visualize nuclei. The central areas of the wounds are shown. At least three fields per section were observed under a fluorescence microscope. Scale bars = 100 μm. (For interpretation of the references to colour in this figure legend, the reader is referred to the web version of this article.)

in a short term. The once every-3-day rhTM-loaded hydrogel, which was composed of 4% gelatin with 0.1% HA and cross-linked by 0.05% EDC, significantly accelerated wound healing compared to rhTM, hydrogel alone, and rhEGF hydrogel. The rhTM hydrogels enhanced granulation tissue formation, re-epithelialization, collagen deposition, and angiogenesis in wound repair. The once every-3-day rhTM hydrogel was stable and drug release was maintained up to 11 months of storage at 4 °C. The developed rhTM hydrogels could meet the needs for clinical practice, and may have future medical applications for wound care especially in diabetic patients.

Declarations of interest

None

Acknowledgments

This work was supported by the Ministry of Science and Technology, Taiwan (MOST 104-2622-B-006-011-CC2 and MOST 105-2622-B-006-005-CC2). The authors would like to thank Blue Blood Biotech Corporation for providing rhTM protein and rhTM indirect ELISA kit.

Appendix A. Supplementary material

Supplementary data to this article can be found online at https://doi.org/10.1016/j.ejpb.2018.12.007.

References

[1] G.C. Gurtner, S. Werner, Y. Barrandon, M.T. Longaker, Wound repair and regeneration, Nature 453 (2008) 314–321.
[2] M. Intelligence, Global Advanced Wound Care Management Market – Segmented by Type of Product and Type of Wound - Growth, Trends, and Forecast (2018–2023), in, 2017.
[3] C. Martin, W.L. Low, M.C. Amin, I. Radecka, P. Raj, K. Kenward, Current trends in the development of wound dressings, biomaterials and devices, Pharm. Pat. Anal. 2 (2013) 341–359.
[4] S.P. Zustiak, Y. Wei, J.B. Leach, Protein-hydrogel interactions in tissue engineering: mechanisms and applications, Tissue Eng. Part B Rev. 19 (2013) 160–171.
[5] K. Skorkowska-Telichowska, M. Czemplik, A. Kulma, J. Szopa, The local treatment and available dressings designed for chronic wounds, J. Am. Acad. Dermatol. 68 (2013) e117–e126.
[6] T. Vermonden, R. Censi, W.E. Hennink, Hydrogels for protein delivery, Chem. Rev. 112 (2012) 2853–2888.
[7] F. Zhang, C. He, L. Cao, W. Feng, H. Wang, X. Mo, J. Wang, Fabrication of gelatin-hyaluronic acid hybrid scaffolds with tunable porous structures for soft tissue engineering, Int. J. Biol. Macromol. 48 (2011) 474–481.
[8] N. Mayet, Y.E. Choonara, P. Kumar, L.K. Tomar, C. Tyagi, L.C. Du Toit, V. Pillay, A comprehensive review of advanced biopolymeric wound healing systems, J. Pharm. Sci. 103 (2014) 2211–2230.
[9] H. Sinno, S. Prakash, Complements and the wound healing cascade: an updated review, Plast. Surg. Int. 2013 (2013) 146764.
[10] N. Pazyar, R. Yaghoobi, E. Rafiee, A. Mehrabian, A. Feily, Skin wound healing and phytomedicine: a review, Skin Pharmacol. Physiol. 27 (2014) 303–310.
[11] Y.H. Li, C.H. Kuo, G.Y. Shi, H.L. Wu, The role of thrombomodulin lectin-like domain in inflammation, J. Biomed. Sci. 19 (2012) 34.
[12] E.M. Conway, Thrombomodulin and its role in inflammation, Semin. Immunopathol. 34 (2012) 107–125.
[13] Y.Y. Hsu, G.Y. Shi, C.H. Kuo, S.L. Liu, C.M. Wu, C.Y. Ma, F.Y. Lin, H.Y. Yang, H.L. Wu, Thrombomodulin is an ezrin-interacting protein that controls epithelial morphology and promotes collective cell migration, FASEB J. 26 (2012) 3440–3452.
[14] H.C. Huang, G.Y. Shi, S.J. Jiang, C.S. Shi, C.M. Wu, H.Y. Yang, H.L. Wu, Thrombomodulin-mediated cell adhesion: involvement of its lectin-like domain, J. Biol. Chem. 278 (2003) 46750–46759.
[15] C.S. Shi, G.Y. Shi, Y.S. Chang, H.S. Han, C.H. Kuo, C. Liu, H.C. Huang, Y.J. Chang, P.S. Chen, H.L. Wu, Evidence of human thrombomodulin domain as a novel angiogenic factor, Circulation 111 (2005) 1627–1636.
[16] C.H. Kuo, M.C. Sung, P.K. Chen, B.I. Chang, F.T. Lee, C.F. Cho, T.T. Hsieh, Y.C. Huang, Y.H. Li, G.Y. Shi, C.Y. Luo, H.L. Wu, FGFR1 mediates recombinant thrombomodulin domain-induced angiogenesis, Cardiovasc. Res. 105 (2015) 107–117.
[17] T.L. Cheng, Y.T. Wu, H.Y. Lin, F.C. Hsu, S.K. Liu, B.I. Chang, W.S. Chen, C.H. Lai, G.Y. Shi, H.L. Wu, Functions of rhomboid family protease RHBDL2 and thrombomodulin in wound healing, J. Invest. Dermatol. 131 (2011) 2486–2494.
[18] T.L. Cheng, Y.T. Wu, C.H. Lai, Y.C. Kao, C.H. Kuo, S.L. Liu, Y.Y. Hsu, P.K. Chen, C.F. Cho, K.C. Wang, W.L. Lin, B.I. Chang, C.M. Chen, H. Weiler, G.Y. Shi, H.L. Wu,

Thrombomodulin regulates keratinocyte differentiation and promotes wound healing, J, Invest. Dermatol. 133 (2013) 1638–1645.
[19] T.L. Cheng, C.H. Lai, P.K. Chen, C.F. Cho, Y.Y. Hsu, K.C. Wang, W.L. Lin, B.I. Chang, S.K. Liu, Y.T. Wu, C.K. Hsu, G.Y. Shi, H.L. Wu, Thrombomodulin promotes diabetic wound healing by regulating toll-like receptor 4 expression, J. Invest. Dermatol. 135 (2015) 1668–1675.
[20] K.H. Chang, H.T. Liao, J.P. Chen, Preparation and characterization of gelatin/hyaluronic acid cryogels for adipose tissue engineering: in vitro and in vivo studies, Acta Biomater. 9 (2013) 9012–9026.
[21] A. Saarai, V. Kasparkova, T. Sedlacek, P. Saha, On the development and characterisation of crosslinked sodium alginate/gelatine hydrogels, J. Mech. Behav. Biomed. Mater. 18 (2013) 152–166.
[22] C. Yang, L. Xu, Y. Zhou, X.M. Zhang, X. Huang, M. Wang, Y. Han, M.L. Zhai, S.C. Wei, J.Q. Li, A green fabrication approach of gelatin/CM-chitosan hybrid hydrogel for wound healing, Carbohydr. Polym. 82 (2010) 1297–1305.
[23] K.K. Wu, Y. Huan, Streptozotocin-induced diabetic models in mice and rats, Curr. Protoc. Pharmacol. (2008) 5–47.
[24] K.K. Chereddy, R. Coco, P.B. Memvanga, B. Ucakar, A. des Rieux, G. Vandermeulen, V. Preat, Combined effect of PLGA and curcumin on wound healing activity, J. Control. Release 171 (2013) 208–215.
[25] S.A. Park, V.K. Raghunathan, N.M. Shah, L. Teixeira, M.J. Motta, J. Covert, R. Dubielzig, M. Schurr, R.R. Isseroff, N.L. Abbott, J. McAnulty, C.J. Murphy, PDGF-BB does not accelerate healing in diabetic mice with splinted skin wounds, PLoS One 9 (2014) e104447.
[26] S.N. Park, J.C. Park, H.O. Kim, M.J. Song, H. Suh, Characterization of porous collagen/hyaluronic acid scaffold modified by 1-ethyl-3-(3-dimethylaminopropyl) carbodiimide cross-linking, Biomaterials 23 (2002) 1205–1212.
[27] M.S. Agren, C.J. Taplin, J.F. Woessner Jr., W.H. Eaglstein, P.M. Mertz, Collagenase in wound healing: effect of wound age and type, J. Invest. Dermatol. 99 (1992) 709–714.
[28] A. Gutierrez-Fernandez, M. Inada, M. Balbin, A. Fueyo, A.S. Pitiot, A. Astudillo, K. Hirose, M. Hirata, S.D. Shapiro, A. Noel, Z. Werb, S.M. Krane, C. Lopez-Otin, X.S. Puente, Increased inflammation delays wound healing in mice deficient in collagenase-2 (MMP-8), FASEB J. 21 (2007) 2580–2591.
[29] B.C. Nwomeh, H.X. Liang, R.F. Diegelmann, I.K. Cohen, D.R. Yager, Dynamics of the matrix metalloproteinases MMP-1 and MMP-8 in acute open human dermal wounds, Wound Repair Regen. 6 (1998) 127–134.
[30] M. Matsui, Y. Tabata, Enhanced angiogenesis by multiple release of platelet-rich plasma contents and basic fibroblast growth factor from gelatin hydrogels, Acta Biomater. 8 (2012) 1792–1801.
[31] R.D. Galiano, J.t. Michaels, M. Dobryansky, J.P. Levine, G.C. Gurtner, Quantitative and reproducible murine model of excisional wound healing, Wound Repair Regen. 12 (2004) 485–492.
[32] W.J. Lindblad, Considerations for selecting the correct animal model for dermal wound-healing studies, J. Biomater. Sci. Polym. Ed. 19 (2008) 1087–1096.
[33] W.Y. Chen, G. Abatangelo, Functions of hyaluronan in wound repair, Wound Repair Regen. 7 (1999) 79–89.
[34] M.G. Neuman, R.M. Nanau, L. Oruna-Sanchez, G. Coto, Hyaluronic acid and wound healing, J. Pharm. Pharm. Sci. 18 (2015) 53–60.
[35] S. Werner, R. Grose, Regulation of wound healing by growth factors and cytokines, Physiol. Rev. 83 (2003) 835–870.
[36] M. Schafer, S. Werner, Cancer as an overhealing wound: an old hypothesis revisited, Nat. Rev. Mol. Cell Biol. 9 (2008) 628–638.
[37] S. Barrientos, O. Stojadinovic, M.S. Golinko, H. Brem, M. Tomic-Canic, Growth factors and cytokines in wound healing, Wound Repair Regen. 16 (2008) 585–601.
[38] H. Hamada, H. Ishii, K. Sakyo, S. Horie, K. Nishiki, M. Kazama, The epidermal growth factor-like domain of recombinant human thrombomodulin exhibits mitogenic activity for Swiss 3T3 cells, Blood 86 (1995) 225–233.
[39] G.K. Kolluru, S.C. Bir, C.G. Kevil, Endothelial dysfunction and diabetes: effects on angiogenesis, vascular remodeling, and wound healing, Int. J. Vasc. Med. 2012 (2012) 918267.
[40] S.Y. Yoo, S.M. Kwon, Angiogenesis and its therapeutic opportunities, Mediat. Inflamm. 2013 (2013) 127170.
[41] P. Martin, Wound healing–aiming for perfect skin regeneration, Science 276 (1997) 75–81.
[42] H.M. DeLisser, M. Christofidou-Solomidou, R.M. Strieter, M.D. Burdick, C.S. Robinson, R.S. Wexler, J.S. Kerr, C. Garlanda, J.R. Merwin, J.A. Madri, S.M. Albelda, Involvement of endothelial PECAM-1/CD31 in angiogenesis, Am. J. Pathol. 151 (1997) 671–677.
[43] J. Asai, H. Takenaka, N. Katoh, S. Kishimoto, Dibutyryl cAMP influences endothelial progenitor cell recruitment during wound neovascularization, J. Invest. Dermatol. 126 (2006) 1159–1167.
[44] J.D. McBride, A.J. Jenkins, X. Liu, B. Zhang, K. Lee, W.L. Berry, R. Janknecht, C.T. Griffin, C.E. Aston, T.J. Lyons, J.J. Tomasek, J.X. Ma, Elevated circulation levels of an antiangiogenic SERPIN in patients with diabetic microvascular complications impair wound healing through suppression of Wnt signaling, J. Invest. Dermatol. 134 (2014) 1725–1734.